

Corrosion Behavior of Ni-Cr Dental Casting Alloys

Porojan Liliana^{1,*}, Savencu Cristina Elena¹, Costea Liviu Virgil², Dan Mircea Laurențiu²,
Porojan Sorin Daniel³

¹ Department of Dental Prostheses Technology (Specialization Dental Technology), Faculty of Dentistry, “V. Babeș” University of Medicine and Pharmacy, Timișoara, Romania

² CAICAM Department, Faculty of Industrial Chemistry and Environmental Engineering, Politehnica University, Timișoara, Romania

³ Department of Oral Rehabilitation (Specialization Dental Technology), Faculty of Dentistry, “V. Babeș” University of Medicine and Pharmacy, Timișoara, Romania

*E-mail: lilianasandu@gmail.com

Received: 22 June 2017 / Accepted: 19 October 2017 / Online Published: 1 December 2017

Nickel–chromium (Ni–Cr) alloys have been used for dental prostheses because of their low prices and excellent properties in veneered restorations. While most Ni-Cr restorations perform well clinically, corrosion products and components of these alloys are known to have the potential to cause hypersensitivity and other tissue reactions. The aim of this study was to investigate the corrosion behavior of four different commercial Ni-Cr dental casting alloys (S1, S2, S3, S4) in simulated oral environment, related to the chemical composition and microstructure, by electrochemical methods, including electrochemical impedance spectroscopy (EIS), chronoamperometric and chronopotentiometric investigation, cyclic voltammetry studies. Samples surface characterization was done using scanning electron microscopy (SEM) before and after immersion in artificial saliva. Corroborating the results of the investigation methods, Ni-Cr alloys represent a suitable alternative for metal frameworks used in prosthetic dentistry. All dental alloys exhibit low corrosion tendency, but S1 and S2 alloys were most stable to corrosion in artificial saliva. The best electrochemical behavior has to be attributed to the composition of the alloys (containing Cr and Mo) and to the compact surface microstructure.

Keywords: Nickel-Chromium dental casting alloys, corrosion behavior, chemical composition, microstructure

1. INTRODUCTION

Nickel–chromium (Ni–Cr) alloys have been used for dental prostheses because of their low prices and excellent properties in veneered restorations. Casting technique is frequently used to obtain

prostheses using Ni–Cr alloys. However, the biocompatibility of Ni-based alloys in an oral environment led to some concerns because of possible allergic reactions to Ni ions [1,2]. By adding different elements the microstructure of Ni-based alloys and their properties can be modified [3]. Cr is commonly used to form a barrier, such that microstructures containing a Cr-rich oxide layer prevent the release of Ni ion from alloys. Beryllium in Ni-based alloys can be used to improve the castability of the alloys and enhance the interaction between porcelain and Ni alloys. For a conventional Ni–Cr alloy system, approximately 20 wt% Cr can be considered as a critical quantity for the compact oxide layer formation of Cr₂O₃ on the surface. Generally, large quantities of loosely stacked oxides, such as NiO or NiCr₂O₄, are observed when the Cr amount is below the critical value [2,4,5].

Even a lot of nickel–chromium restorations have a good clinical performance over time, corrosion products and components of these base metal alloys are known to have the potential to cause hypersensitivity or different tissue reactions [6,7].

It is important that corrosion and metal ion release from these alloys be reduced as much as possible [8].

Corrosion properties of Ni–Cr alloys depend on their composition, microstructure and forming of a passive film layer [9,10]. Experimental studies showed that alloys with 16–27% Cr, 6–17% Mo, and no Be display homogeneous protective oxides surface, low corrosion rates, and large passivation ranges. Be containing alloys exhibit higher corrosion rates, and smaller passivation ranges, as compared to non-Be containing alloys [11-14]. Understanding and evaluating the corrosion behavior of Ni–Cr dental alloys in the oral environment is important for understanding their biocompatibility and clinical performance, represented by health benefit–risks of these alloys.

Various in vitro methods have been used to evaluate quantitatively the corrosion behavior of biomaterials. Electrolytes like 1% NaCl, Fusayama's artificial saliva, Darvells solution were used for electrochemical and potentiodynamic polarization methods in order to evaluate the corrosion rate and corrosion resistance [15,16]. Surface analysis like X-ray photoelectron spectroscopy has also been used to complete studies [17].

Potentiodynamic polarization method is an acceleration test, which helps manufacturers to evaluate dental casting alloys in a short time, and to provide information regarding the corrosion behavior of the alloys for the practitioners [18].

2. PURPOSE

The aim of this study was to investigate corrosion behavior of four different commercial Nickel-Chromium cast dental alloys in simulated oral environment, related to their chemical composition and microstructure.

3. EXPERIMENTAL

Samples of 3 mm thickness and 15 mm diameter were produced by conventional casting technique from four different commercial Ni–Cr alloys, following manufacturers' indications. The

detailed composition in wt%, of the materials employed in the present research, as mentioned by the manufacturer, is detailed in Table 1. Wax-ups were manufactured with the specified dimensions, and the conventional lost wax technique has been used. A phosphate-bonded investment Bellavest SH (Bego, Bremen, Germany) was chosen for investing and the mold was then cast with the investigated Ni-Cr alloys at 900°C using a vacuum pressure casting machine Nautilus (Bego, Bremen, Germany). After cooling down to room temperature, the specimens were divested, sandblasted with alumina particles (200 µm) and finished with rotative instruments, burs suitable for the processed alloys.

Table 1. Composition of the investigated alloys.

Sample	Compozition (%weight)
S1	Ni 65, Cr 22.,5, Mo 9.5, Nb, Si, Fe, Ce
S2	Ni 64.5, Cr 22, Mo 10, Si 2.1, Nb, Mn, B
S3	Ni 66, Cr 26.5, Mo 5, Si 1.5, < 1% Mn, B
S4	Ni 61.4, Cr 25.9, Mo 11, Si 1.5, others < 0.1%

Samples were finished further-more with silicon carbide of successively lower graining and 1µm grit diamond paste respectively, degreased in ethanol and finally sonicated in distilled water, rinsed and dried before being used in the electrochemical tests. Surface morphology of the samples has been characterized by scanning electron microscopy (SEM) using a FEI INSPECT S microscope before as well as after performing the electrochemical corrosion testing.

The probes used as working electrodes have been fixed in a specially designed Teflon holder, exposing only one side of the sample towards the electrolyte solution.

The electrolyte solution used for all electrochemical measurements was modified Fusayama artificial saliva with the composition detailed in Table 2. All reagents used were employed as purchased with no further purification. All the listed components are dissolved in bidistilled water and the pH value has been adjusted at the desired value using lactic acid. Corrosion tests were performed at room temperature and pressure.

Table 2. Composition of the employed artificial saliva (modified Fusayama formulation):

Component	Concentration [g.L ⁻¹]
NaCl	0.4
KCl	0.4
CaCl ₂ .2H ₂ O	0.795
NaH ₂ PO ₄ .H ₂ O	0.690
Na ₂ S.9H ₂ O	0.005
Urea	1.0
KSCN	0.3

Electrochemical measurements were carried out using a BioLogic SP150 potentiostat/galvanostat in a conventional three-electrode cell system. The investigated dental alloys prepared samples were successively used as working electrodes. The counter electrodes consisted of two graphite rods, and Ag/AgCl acted as reference electrode. All potentials are referred to the saturated Ag/AgCl reference electrode ($E_{\text{Ag/AgCl}} = 0.197 \text{ V/NHE}$).

The employed electrolyte solution within all the experiments with the aim of determining the corrosion potential as well as the corrosion current of the studied substrates consisted of modified Fusayama artificial saliva. In order to closely simulate the physiological conditions in the oral cavity, the solution was kept at $37 \pm 1^\circ\text{C}$ and pH of 5. The solution was changed with a fresh one after each performed experiment. The electrochemical behaviour of the tested materials in artificial saliva was investigated by cyclic voltammetry. Linear sweep voltammetry (Tafel method) and electrochemical impedance spectroscopy as well as chronoamperometry and chronopotentiometry have been employed in order to get a better insight regarding the corrosion processes of the studied metal alloys.

To determine open circuit potential of the investigated dental alloys chronopotentiometric method has been applied. Variation of the electrode potential was recorded over a period of 60 minutes. This time is considered to be optimal for reaching an equilibrium or quasi-state at the electrode - solution interface as a preliminary step before commencing the corrosion studies through the Tafel method [19].

Electrochemical impedance spectroscopy (EIS) investigations have been conducted using a BioLogic SP150 potentiostat/galvanostat equipped with an EIS module, within the frequency layoff of 10 mHz and 100 kHz, the amplitude of the alternating voltage was of 10 mV. A number of 60 points have been recorded for each spectrum with a logarithmic distribution of 10 points per decade. The experimental data has been fitted using the ZView – Scribner Associates Inc. software and equivalent electrical circuits by applying the Levenberg – Marquardt least squares complex non-linear fitting algorithm.

In order to undertake a thorough electrochemical analysis and in pursuance for accomplishing a comprehensive characterization of the corrosion processes taking place at the surface of the four considered dental alloys, chronoamperometric determinations have been conducted followed by potentiometric measurements. The possible development of a passivating film coating on the electrode surface leads to an increase in corrosion resistance of the studied dental alloys. Chronoamperometry investigations have been performed at two potential values relative to OCP, namely +25 mV/OCP and +250 mV/OCP, respectively for a period of 15 minutes. The shift of the electrode potential after electrochemical oxidations has been recorded chronopotentiometrically at $I = 0 \text{ A}$ for 15 minutes, long enough for the quasi-stable steady state to occur at the electrode - solution interface.

A comprehensive characterization of the processes taking place at the electrode (i.e. the studied dental alloy) - solution interface (artificial saliva) has been performed by investigating the electrochemical behavior of the studied alloys in the testing medium over a fairly large potential window. The anodic limit has been set by the anodic oxygen formation whereas the cathodic limit was given by the reductive hydrogen formation.

Samples surface characterization was done using scanning electron microscopy (SEM) before and after immersion in artificial saliva.

4. RESULTS AND DISCUSSION

The variation of the open circuit potential for the four studied dental alloys in artificial saliva over time is shown in Figure 1.

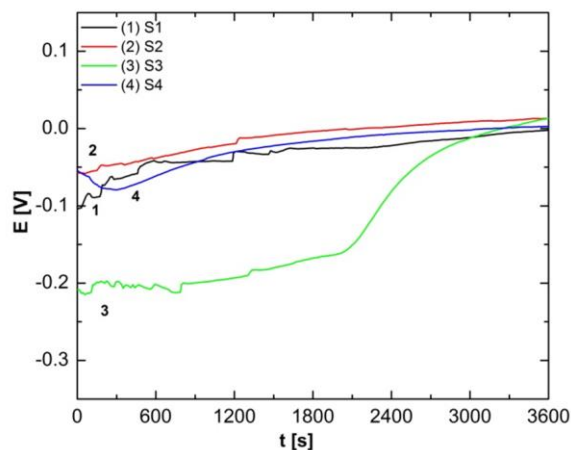


Figure 1. Open circuit potential evolution for the investigated samples in artificial saliva: S1, S2, S3, S4.

The potential variation over time can offer some relevant information regarding the corrosion mechanism of the studied materials. According to the chronoamperometric results presented in Fig. 1, it can be observed that after a scanning period of 60 minutes, all the investigated systems reached a quasi-steady state. It can be seen that the potentials of all the studied electrode materials are on an ascending trend in the first part of the recording period before reaching their equilibrium values. The most notable aspect consists in the sudden increase of the much more negative electrode potential of S3 after about 35 minutes, followed by its stabilization within the same region as all the other studied probes, thus exhibiting similar corrosion resistance.

Open-circuit potential (OCP) allows an information regarding the relative noble behavior of the studied alloys, related to the electrolyte under consideration, being a measurement of the corrosion tendency. Lower OCP values represent a greater tendency toward corrosion. An increase in the electrochemical potential during immersion can usually be attributed to thickening of the passive film, which becomes more protective. After 50 minutes of immersion, all of the alloys tended to achieve a steady state. Even among the different alloys there were no significant differences in the electrochemical potential.

Tafel polarization curves recorded for the investigated metal alloy samples using artificial saliva (modified Fusayama formulation) as electrolyte, at a constant temperature of 37°C are depicted in Fig. 2. The scans have been performed within a potential window delimited by a cathodic potential of -250 mV/OCP and an anodic potential of +250 mV/OCP respectively. The obtained potentiodynamic dependencies have been fitted using the Bio-Logic EC-Lab[®] software package, in order to determine key parameters for each of the four tested samples like: corrosion current density (i_{corr}), corrosion potential (E_{corr}), cathodic and anodic Tafel slopes (b_c and b_a), polarization resistance (R_p) and corrosion rate (v_{cor}) respectively, the obtained data being summarized in Table 3.

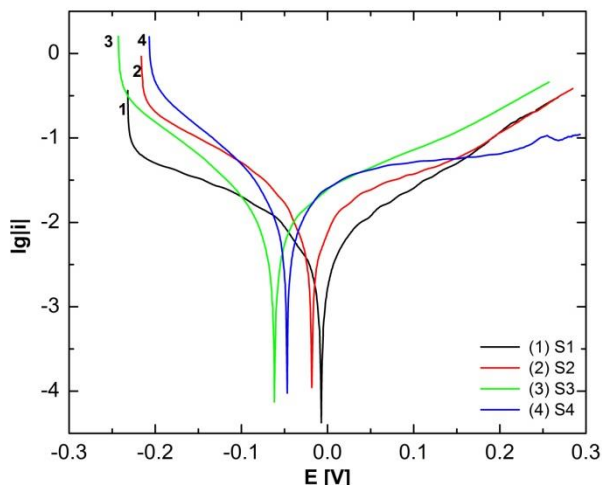


Figure 2. Linear polarization curves for the studied alloys in artificial saliva, at 37°C and a scan rate of 1 mV·s⁻¹.

Table 3. Corrosion parameter data for the investigated dental alloys in artificial saliva.

Samples	T [°C]	i_{cor} [$\mu\text{A cm}^{-2}$]	E_{cor} [mV]	$-b_c$ [$\text{mV}\cdot\text{dec}^{-1}$]	b_a [$\text{mV}\cdot\text{dec}^{-1}$]	R_p [$\text{k}\Omega$]	$v_{corr} \cdot 10^3$ [$\text{mm}\cdot\text{year}^{-1}$]
S1	37	0.426	-8.61	160.1	181.2	57.32	6.50
S2		0.966	-14.75	223.1	146.1	26.15	14.56
S3		0.876	-57.74	185.3	122.7	29.20	13.11
S4		1.224	-50.16	231.5	103.1	15.16	17.78

The polarization curves made for tested alloys confirm the results of open circuits potential test, with a higher rate of corrosion for S3.

Evaluating the potentiodynamic polarization curves, the first important observation is that all of the studied alloys could form a passive film, as indicated by the plate route plateau where an increase in corrosion potential (E_{corr}) had no significant influence on the current density (i_{corr}). The current density was similar for the evaluated alloys. The length of the passive plateau was variable, and a transpassive region could be observed for all of the alloys [20]. A higher corrosion current density indicates that the overall corrosion rate will be higher.

The electrochemical impedance spectra have been recorded in order to investigate the corrosion processes occurring on the surface of the tested dental alloys in artificial saliva at 37°C at the corresponding corrosion potentials (E_{corr}) listed in Table 3. The obtained results are shown in Figs. 3 and 4 as Nyquist and Bode plots respectively.

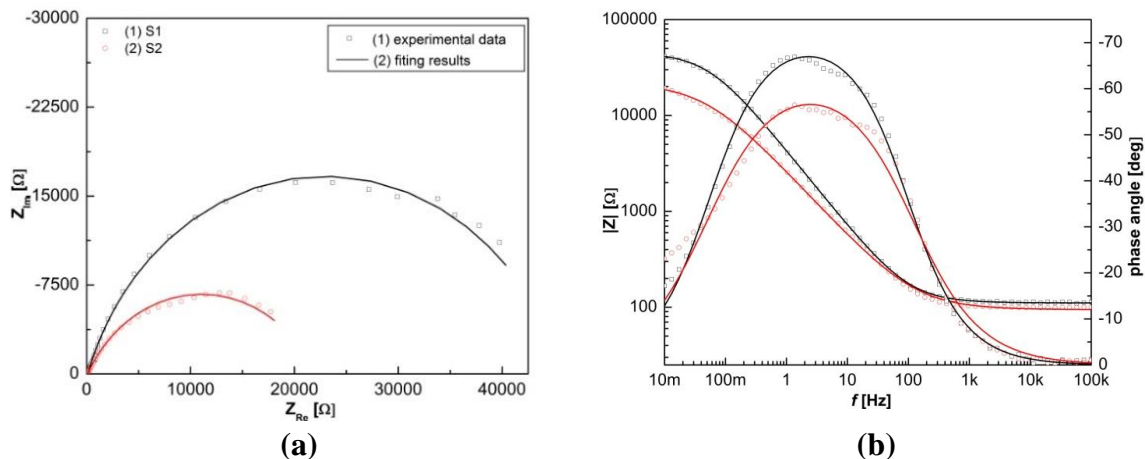


Figure 3. Nyquist (a) and Bode plots (b) recorded on samples 1 and 2 in artificial saliva.

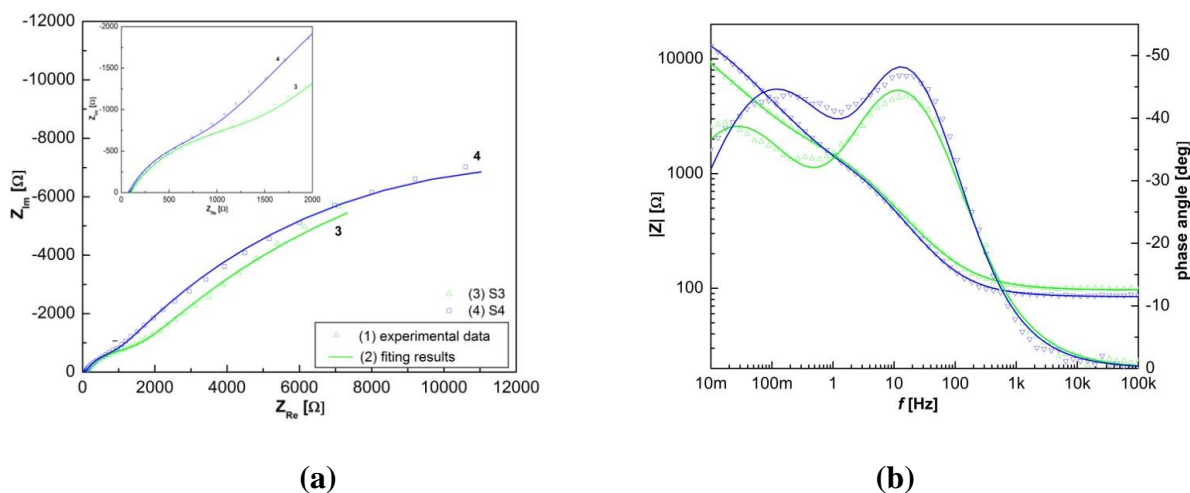


Figure 4. Nyquist (a) and Bode plots (b) recorded on samples 3 and 4 in artificial saliva.

EIS data were fitted using a complex non-linear least squares (CNLS) procedure with the equivalent electrical circuits shown in Fig. 5a for S1 and S2, and Fig. 5b for S3 and S4. Calculated values of the circuit elements for the corrosion processes are listed in Tables 4 and 5.

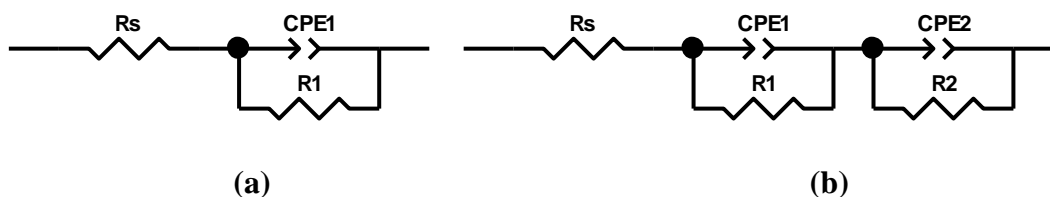


Figure 5. Proposed electrical circuits used for modeling the corrosion process for S1 and S3 (a), S3 and S4 (b) in artificial saliva.

Table 4. Calculated values of the circuit elements for the corrosion process of S1 and S2.

Samples	R_s [$\Omega \text{ cm}^2$]	$T \cdot 10^5$ [$\text{F cm}^{-2} \text{ s}^{n-1}$]	n	R_{ct} [$\text{k}\Omega \text{ cm}^2$]	$\text{Chi}^2 \cdot 10^3$
S1	111	5.21	0.81	45.6	2.5
S2	94.4	9.3	0.78	22.2	5.0

Table 5. Calculated values of the circuit elements for the corrosion process of S3 and S4.

Samples	R_s [$\Omega \text{ cm}^2$]	$T_1 \cdot 10^4$ [$\text{F cm}^{-2} \text{ s}^{n-1}$]	n_1	R_{ct1} [$\text{k}\Omega \text{ cm}^2$]	$T_2 \cdot 10^4$ [$\text{F cm}^{-2} \text{ s}^{n-1}$]	n_2	R_{ct2} [$\text{k}\Omega \text{ cm}^2$]	$\text{Chi}^2 \cdot 10^3$
S3	96.7	1.26	0.77	1.17	5.43	0.63	21.9	1.8
S4	84.7	1.13	0.82	0.65	3.16	0.68	20.0	2.1

The total charge transfer resistance values for all samples investigated in the present corrosion studies in artificial saliva are presented in Table 6.

Table 6. Calculated total charge transfer resistances (R_{ct}) of tested samples for corrosion process in artificial saliva.

Sample	R_{ct} [$\text{k}\Omega \text{ cm}^2$]
S1	45.6
S2	22.2
S3	23.1
S4	20.7

Figure 6 shows the graphical results obtained after the chronoamperometric studies recorded at $E_{ox} = +25 \text{ mV/OCP}$ followed by the OCP variation for the investigated materials.

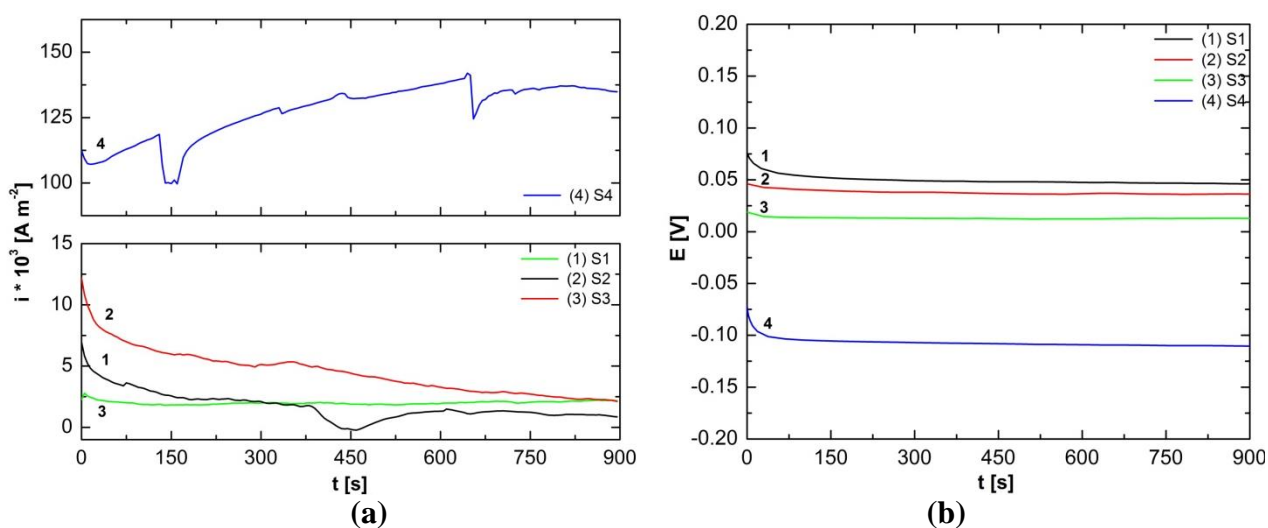


Figure 6. Chronoamperometric measurements followed by chronopotentiometric data at $I = 0 \text{ A}$ for electrochemical oxidation at $+25 \text{ mV/OCP}$ (a) and after the oxidation step (b).

Analysis of the data presented in Fig. 6 reveals that the four samples exhibit different oxidation behavior. A passivating physically adherent oxide layer is formed on the exposed surface of S1, S2 and S3 evidenced by the steady decrease of current densities during oxidation. This process is more pregnant on the surface of the S1 and S2 alloys. The formed oxide coating provides the before mentioned substrates anticorrosive protection. Although one cannot observe a significant decrease of current density on the timescale of the experiments, the relatively small variation of this parameter can be used as an indicator for the formation of a passivating coating as well as for the increase of its thickness. The low value of the current density after 15 minutes, comparable with that recorded for S2, denotes a degree of protection against corrosion provided to the dental material by the oxide layer, at least at this value of the oxidation potential. S4 delivers a somehow different oxidation behavior with a steady increase of the current densities, indicating a continuous oxidation of the investigated alloy. The formed oxide layer are most probably loose, weakly adherent on the alloy surface, presumably showing a porous structure, allowing the substrate to being further exposed to oxidation, thus increasing the rate of corrosion. Variation of the open circuit potential for the investigated electrode materials after the oxidation step shows a stabilization of the electrode potentials.

Fig. 7 shows the graphical results obtained after the chronoamperometric studies recorded at $E_{ox} = +250$ mV/OCP followed by the OCP variation for the four investigated materials, which are listed in Table 7.

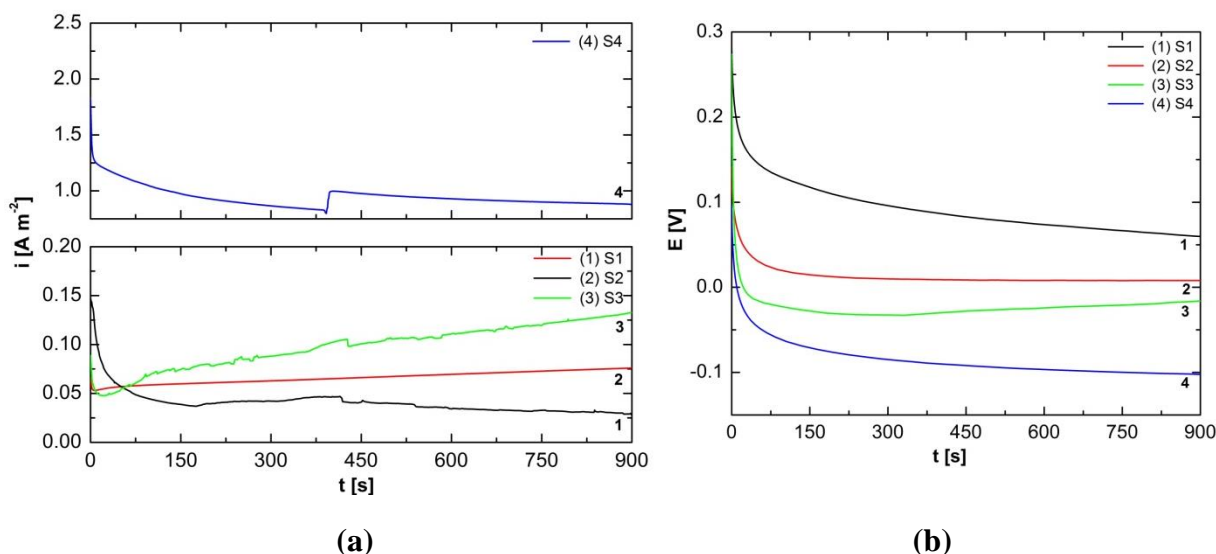


Figure 7. Chronoamperometric measurements followed by chronopotentiometric data at $I = 0$ A for electrochemical oxidation at +250 mV/OCP (a) and after the oxidation step (b).

Table 7. Chronoamperometric and cronopotentiometric data for the investigated dental alloys in artificial saliva.

Samples	Chroamperometric data		Chropotentiometric data		
	i_1 [mA m ⁻²]	i_2 [A m ⁻²]	E_{OCP} [mV]	E_1 [mV]	E_2 [mV]
S1	0.86	0.028	-2.12	46.4	59.7
S2	2.12	0.076	13.8	36.2	7.8
S3	2.18	0.135	13.1	12.8	-16.4
S4	135	0.877	2.7	-111	-102

Calculated values of the circuit elements in artificial saliva after electrochemical oxidation are presented in Tables 8 and 9.

Table 8. Calculated values of the circuit elements on samples 1 and 2 corrosion process in artificial saliva after electrochemical oxidation:

Samples	R_s [$\Omega \text{ cm}^2$]	$T \cdot 10^5$ [$\text{F cm}^{-2} \text{ s}^{-1}$]	n	R_{ct} [$\text{k}\Omega \text{ cm}^2$]	$\text{Chi}^2 \cdot 10^3$
S1	102	4.0	0.86	64.4	2.5
S2	95.4	10.3	0.71	30.6	5.0

Table 9. Calculated values of the circuit elements on samples 3 and 4 corrosion process in artificial saliva after electrochemical oxidation:

Samples	R_s [$\Omega \text{ cm}^2$]	$T_1 \cdot 10^4$ [$\text{F cm}^{-2} \text{ s}^{-1}$]	n_1	R_{ct1} [$\text{k}\Omega \text{ cm}^2$]	$T_2 \cdot 10^4$ [$\text{F cm}^{-2} \text{ s}^{-1}$]	n_2	R_{ct2} [$\text{k}\Omega \text{ cm}^2$]	$\text{Chi}^2 \cdot 10^3$
S3	92.4	1.36	0.76	0.86	8.38	0.66	19.8	0.8
S4	114	1.25	0.74	0.44	11.0	0.74	5.92	0.9

The total charge transfer resistance values for all samples investigated in the present corrosion studies in artificial saliva before and after electrochemical oxidation at +250 mV/OCP are presented in Table 10.

Table 10. Calculated total charge transfer resistances (R_{ct}) of tested samples for corrosion process in artificial saliva before (E_{corr}) and after electrochemical oxidation at +250 mV/OCP (E_2).

Samples	R_{ct} [$\text{k}\Omega \text{ cm}^2$]	R_{ct-ox} [$\Omega \text{ cm}^2$]
S1	45.6	64.4
S2	22.2	30.6
S3	23.1	20.7
S4	20.7	6.36

The comparative display of the cyclic voltammograms for the four studied electrode substrates is shown in Fig. 8. Each scan has been performed at a sweep rate of 100 mV s^{-1} , starting from the open circuit potential towards anodic oxidation.

Analyzing the voltammograms presented in Fig. 8, some observations can be assumed. The probes manufactured of S1 and S2 are the most stable to corrosion in the chosen reaction medium (i.e. artificial saliva). Only a relative small current increase of about 2 A m^{-2} is recorded on a potential range between +0.25 and +0.80 V vs. ref. This increase can be attributed to the formation on the surface of the two electrodes of a passivation coating. Switching the scan direction towards the cathodic region does not reveal a similar counterpart of the above mentioned current increase. This shoulder would have been caused by the dissolution of the passivating film formed during the anodic scan. This leads us to the assumption that the passivating coating is adherent to the electrode surface of both materials, electrochemically stable in artificial saliva and, most important, shows a protective

effect against corrosion. The latter aspect, highlighted by the electrochemical impedance studies performed before and after chromoamperometry, is responsible for a higher corrosion resistance shown by the two dental alloys.

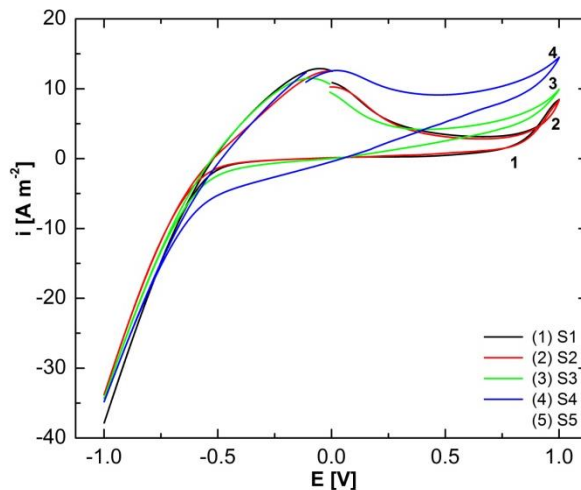


Figure 8. Cyclic voltammograms recorded on the studied dental alloy samples in artificial saliva scan rate: 100 mV s^{-1} .

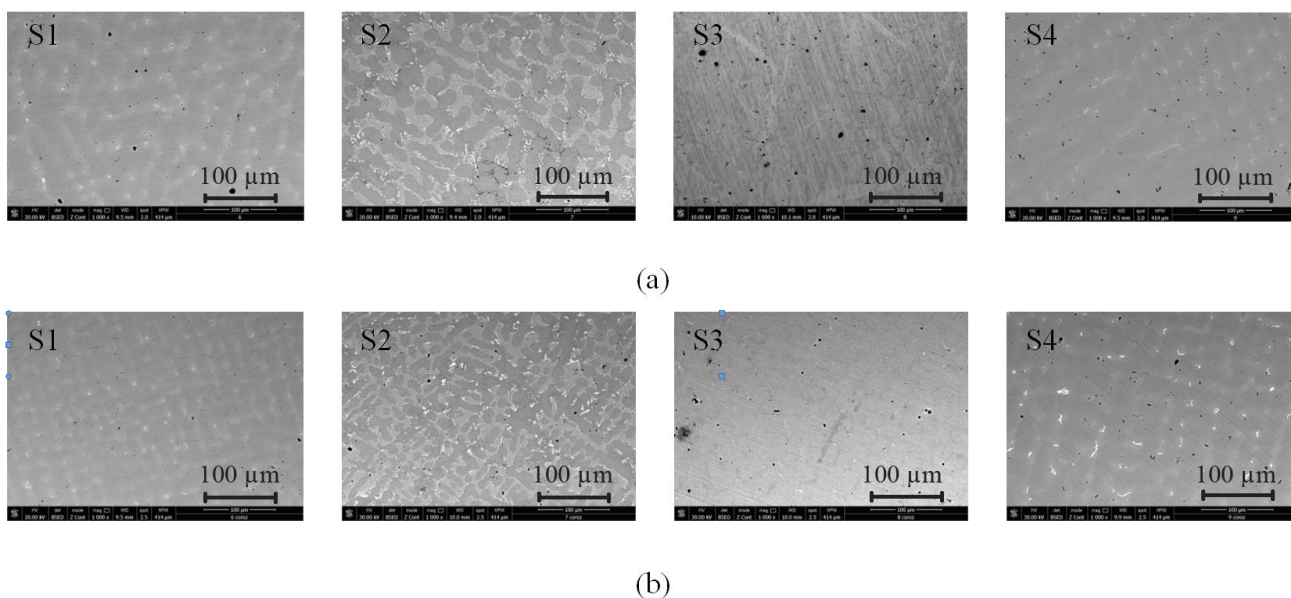


Figure 9. SEM pictures of alloy the alloys before (a) and after (b) corrosion.

The samples consisting of S3 and S4 are much more susceptible of undergoing electrochemical oxidation processes. Current densities of about 5 and 10 A m^{-2} have been recorded for the two alloys respectively, over the same anodic potential range. This comes as an indication for the forming and further development of an oxide film on the electrode surface but also suggests a constant dissolution of these alloys as well. Scanning towards more negative potentials reveals a current increase on the S4

alloy, corresponding to the one obtained on the anodic scan, but of lower intensity. This behavior can be assigned to the dissolution process of the oxide layer formed on the alloy surface during the cathodic reduction of the metal components.

Samples surface characterization was done using scanning electron microscopy (SEM) (Fig. 9) before and after immersion in artificial saliva.

The alloys are characterized by a solid phase solution array in dendritic disposition and an interdendritic phase regularly distributed. A higher volume of interdendritic arrangement was observed at S2. The most casting defects as voids are present in S3 and S4.

Corrosion of Ni-Cr alloys is a complex process, depending on many factors, like the composition, microstructure, processing method, surface treatment, and oral environment [21-25]. Recent studies show that the Lipopolysaccharides, constituents of gingival crevicular fluid and may affect negatively the electrochemical behavior of base metal alloys [26]. Because the use of tooth bleaching agents became increasingly popular, the corrosion resistances of Ni-Cr alloys in different concentrations of H_2O_2 were studied and it was demonstrated that bleach will promote the corrosion of the alloys [27]

Different alloying elements may influence the corrosion behavior, resulting in release of elements into the electrolytes and accordingly increasing or decreasing the corrosion rate [9, 21, 28, 29]. Many studies of passivation and the compositions of passive oxide films have been reported for Ni-Cr and Ni-Cr-Mo alloys [30]. Chromium oxide (Cr_2O_3) and molybdenum oxide (MO_3) provide the initial stability to prevent dissolution of metal ions and so induce resistance to corrosion and a lower corrosive rate. The composition and integrity of the surface oxide film on Ni-Cr dental casting alloy are critical for their clinical performance. The results of different studies showed that Ni-Cr casting alloys with a higher chromium and molybdenum content have much higher passive range and are immune to corrosion. This depends not only on the chemical composition but also on the characterization of passive film on the alloys [31].

5. CONCLUSIONS

After electrochemical techniques were used to assess the electrochemical behavior of different commercial Ni-Cr cast dental alloys and within the limitation of this study it can be concluded that:

- The potential variation over time can offer some relevant information regarding the corrosion mechanism of the Ni-Cr alloys. Recorded open circuit potentials reflect a low corrosion tendency, similar for S1, S2 and S3 and higher for S4. An increase in the electrochemical potential for all alloys during immersion can be attributed to thickening of the passive film, which becomes more protective.
- The polarization curves made for tested alloys confirm the results of open circuits potential test, with a higher rate of corrosion for S4.
- Chronoamperometric and chronopotentiometric investigations revealed different oxidation behavior. A passivating physically adherent oxide layer is formed on the exposed surface of S1, S2 and S3, more pregnant on the surface of the S1 and S2 alloys. The formed oxide coating

provides the before mentioned substrates anticorrosive protection. S4 delivers an increase of the current densities, indicating a continuous oxidation of the investigated alloy. The formed oxide layer are most probably loose, weakly adherent on the alloy surface, presumably showing a porous structure, allowing the substrate to being further exposed to oxidation, thus increasing the rate of corrosion.

- The comparative display of the cyclic voltammograms show that the probes manufactured of S1 and S2 are the most stable to corrosion in the artificial saliva. The samples consisting of S3 and S4 are much more susceptible of undergoing electrochemical oxidation processes.

- Corroborating the results of the investigation methods, Nickel-Chromium alloys represent a suitable alternative for metal frameworks used in prosthetic dentistry. All dental alloys exhibit low corrosion tendency, but S1 and S2 alloys were most stable to corrosion in artificial saliva.

- The best electrochemical behavior has to be attributed to the composition of the alloys (containing Cr and Mo) with a compact surface structure.

References

1. C.M. Wylie, R.M. Shelton, G.J.P. Fleming, A.J. Davenport, *Dent. Mater.*, 23 (2007) 714.
2. W.C. Chen, F.Y. Teng, C.C. Hung, *Mater. Sci. Eng. C Mater. Biol. Appl.*, 35 (2014) 231.
3. D.M. Sarantopoulos, K.A. Beck, R. Holsen, D.W. Berzins, *J. Prosthet. Dent.*, 105(1) (2011) 35.
4. M. Sennour, L. Marchetti, F. Martin, S. Perrin, R. Molins, M. Pijolat, *J. Nucl. Mater.*, 402 (2-3) (2010) 147.
5. J.R. Bauer, A.D. Loguercio, A. Reis, L.E. Rodrigues Filho, *Braz. Oral. Res.*, 20(1) (2006) 40.
6. J.C. Setcos, A. Babaei-Mahani, L.D. Silvio, I.A. Mjor, N.H. Wilson, *Dent. Mater.*, 6 (2006) 133.
7. D.A. Moneret-Vautrin, D. Burnel, J. Sainte-Laudy, E. Beaudouin, A. Croizier, *Allerg. Immunol.*, 36 (2004) 311.
8. H.Y. Lin, B. Bowers, J.T. Wolan, Z. Cai, J.D. Bumgardner, *Dent. Mater.*, 24(3) (2008) 378.
9. H.H. Huang, *Biomaterials*, 24(9) (2003) 1575.
10. M.D. Roach, J.T. Wolan, D.E. Parsell, J.D. Bumgardner, *J. Prosthet. Dent.*, 84(6) (2000) 623.
11. H.H. Huang, *J. Biomed. Mater. Res.*, 60(3) (2002) 458.
12. J.D. Bumgardner, L.C. Lucas, *J. Dent. Res.*, 74(8) (1995) 1521.
13. J.D. Bumgardner, L.C. Lucas, *Dent. Mater.*, 9(4) (1993) 252.
14. J.D. Bumgardner, L.C. Lucas, *J. Appl. Biomater.*, 5(3) (1994) 203.
15. R.I. Holland, *Scand. J. Dent. Res.*, 99(1) (1991) 75.
16. M.D. Roach, J.T. Wolan, D.E. Parsell, J.D. Bumgardner, *J. Prosthet. Dent.*, 84(6) (2000) 623.
17. J.C. Wataha, C.T. Malcolm, C.T. Hanks, *Int. J. Prosthodont.*, 8(1) (1995) 9.
18. J. Geis-Gerstorfer, K.H. Sauer, K. Passler, *Int. J. Prosthodont.*, 4(2) (1991) 152.
19. A. Łukaszczyk, J. Augustyn-Pieniążek, *Arch. Metall. Mater.*, 60(1) (2015) 523.
20. R. Galo, L.A. Rocha, A.C. Faria, R.R. Silveira, R.F. Ribeiro, G. de Mattos, *Mater. Sci. Eng. C Mater. Biol. Appl.*, 45 (2014) 519.
21. J.C. Wataha, *J. Prosthet. Dent.*, 83(2) (2000) 223.
22. S.P. Kedici, A. Abbas Aksut, M. Ali Kilicarslan, G. Bayramoglu, K. Gokdemir, *J. Oral. Rehab.*, 25(10) (1998) 800.
23. A.S. Al-Hiyasat, O.M. Bashabsheh, H. Darmani, *Int. J. Prosthodont.*, 15(5) (2002) 473.
24. C.C. Chen, R.G.S. Chen, S.T. Huang, *J. Biomed. Mater. Res.*, 60(3) (2002) 458.
25. G. Schmalz, P. Garhammer, *Dent. Mater.*, 18(5) (2002) 396.

26. W. Yu, C. Qian, W. Weng, Songmei Zhang, *J. Prosthet. Dent.*, 116(2) (2016) 286.
27. M.F. He, H. Wang, H. Jiang, S. Zhao, D. Pan, *Trans. Nonferrous Met. Soc. China.*, 26(5) (2016) 1353.
28. M. Syverud, J.E. Dahl, H. Herø, E. Morisbak, *Dent. Mater.* 17(1) (2001) 7.
29. R.G. Craig, F.A. Peyton, *Restorative Dental Materials*, Mosby, (1975) St. Louis, Mo, USA.
30. A.C. Lloyd, J.J. Noël, S. McIntyre, D.W. Shoesmith, *Electrochim. Acta.*, 49(17) (2014) 3015.
31. S.B. Rao, R. Chowdhary, *Int. J. Dent.*, (2011) ID 397029.

© 2018 The Authors. Published by ESG (www.electrochemsci.org). This article is an open access article distributed under the terms and conditions of the Creative Commons Attribution license (<http://creativecommons.org/licenses/by/4.0/>).